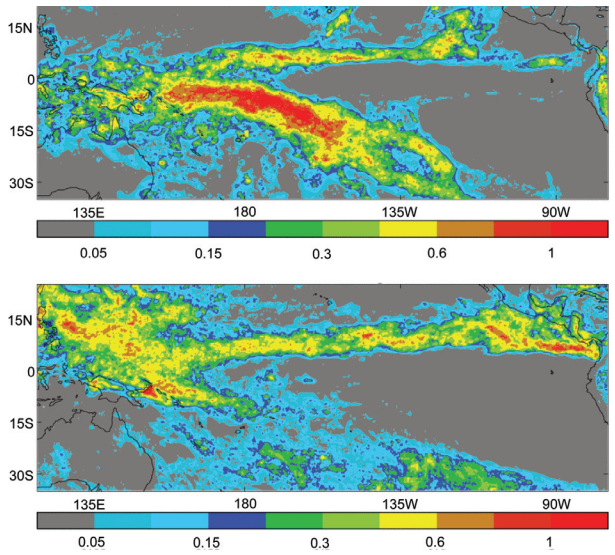

Fig. 4.25. Average rainfall rate (mm h^{-1}) from TRMM 0.25° analysis for (top) February and (bottom) August 2005. Contours are unevenly spaced at 0.05, 0.10, 0.15, 0.20, 0.30, 0.40, 0.60, 0.80, and 1.00 mm h^{-1}.

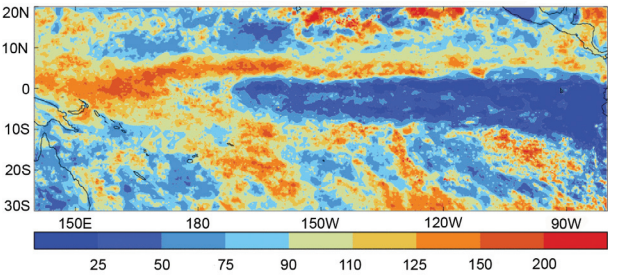

Fig. 4.26. Annual average rainfall rate (mm h^{-1}) from TRMM 0.25° analysis for 2005, as a percentage of the 1998–2004 mean.

For the year as a whole, high-resolution TRMM rainfall data (0.25° latitude × 0.25° longitude grid) suggest that precipitation was slightly above the 1998–2004 average in the northern ITCZ (Fig. 4.26), and also in the southern ITCZ and SPCZ to about 160°W.

5. THE POLES—A. M. Waple[89], Ed.

a. Overview—A. M. Waple[89] and J. Richter-Menge[74]

The permanent presence of sea ice, ice sheets, and continuous permafrost are unique features of the polar regions. The Arctic is further distinguished because it sustains human and wildlife populations in a harsh environment, as documented in the Arctic Climate Impact Assessment published in November 2004 (online at www.acia.uaf.edu). These characteristics amplify the impact of climate change on the region's physical, ecological, and societal systems. Such impacts reach beyond the Arctic region. For instance, studies are underway to determine the extent to which the loss of sea ice cover and the conversion of tundra to larger shrubs and wetlands, observed to have occurred over the last two decades, have impacted multiyear persistence in the surface temperature fields, especially in the Pacific sector.

In this section, observations that indicate continuing trends in the current state of physical components of the Arctic system, including the atmosphere, ocean, sea ice cover, and land, are discussed. The temporal extent of the data provides a multidecadal perspective and confirms the sensitivity of the Arctic to changes in the global climate system. The destabilization of several known relationships between climate indices (e.g., Arctic Oscillation) and Arctic physical system characteristics (e.g., continued reduced sea ice cover and increased greenness of the tundra) presents an intriguing and significant puzzle with respect to the contemporary global climate system.

It was one of the warmest years on record for Greenland, with an especially warm and foggy spring. Surface temperature and ice melt are discussed for Greenland in the context of a warming trend over the nation.

Also, trends and observations in temperature, sea ice, and stratospheric ozone depletion are discussed with respect to Antarctica. As the continent with more than 70% of Earth's freshwater storage, trends in Antarctic climate are of critical importance in determining the long-term impact of climate change.

b. Arctic—J. Richter-Menge,[74] J. Overland,[62] A. Proshutinsky,[68] V. Romanovsky,[77] J. C. Gascard,[25] M. Karcher,[37] J. Maslanik,[52] D. Perovich,[66] A. Shiklomanov,[83] and D. Walker[87]

1) Atmosphere

(i) Circulation regime

The annually averaged AO index in 2005 was slightly negative, continuing the trend of a relatively low and fluctuating index that began in the mid-1990s (Fig. 5.1). This follows a strong positive pattern from 1989 to 1995. Current characteristics of the AO are more consistent with the period from the 1950s to the 1980s, when the AO switched frequently between positive and negative phases.

(ii) Surface temperatures

In 2005, annual average surface temperatures over land areas north of 60°N remained above the mean value for the twentieth century (Fig. 5.2), as they have since the early 1990s. Figure 5.2 also shows warm temperatures in the 1930s and early 1940s, possibly suggesting a longer-term oscillation in climate. However, a detailed analysis shows different proximate

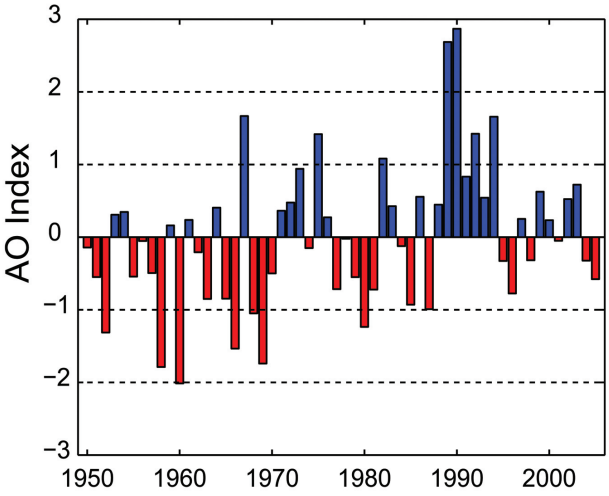

Fig. 5.1. Time series of the annually averaged AO Index for the period 1950–2005, based on data from the following Web site: www.cpc.ncep.noaa.gov. [Courtesy: I. Rigor]

causes and characteristics for the 1930s compared to the 1990s maxima. The early warm anomalies appear to be characterized by large region-to-region differences and are limited to high latitudes (Johannessen et al. 2004; Overland et al. 2004). The warm anomalies since the 1990s tend to be Arctic-wide and reach into the midlatitudes.

Near-surface air temperatures in boreal winter and spring 2005 continued to have the same general spatial pattern of warm anomalies as that of 2000–04 (Fig. 5.3a). The first major feature is positive (warm) anomalies over the entire Arctic, consistent with Fig. 5.2. The second feature is the strong maxima north of eastern Siberia and around the Davis Strait. Spring anomalies (March–June) over the last 6 yr for these coastal areas are near 3°–4°C. The region north of eastern Siberia is also a main location for loss of sea ice cover over the last decade. While the Arctic-wide pattern of positive anomalies was established in the early 1990s, the locations of the 2000–05 temperature anomaly maxima (consistent with the 2005 pattern shown in Fig. 5.3a) contrast with those of the early 1990s (Fig. 5.3b).

The current pattern of near-surface temperature anomalies (2000–05) is distinctly different from the near-surface temperature anomaly patterns associated with the two major atmospheric circulation patterns that characterized the second half of the twentieth century (Quaddrelli and Wallace 2004). The positive phases of these patterns were present during 1989–95 (Fig. 5.3b) and 1977–88 (Fig. 5.3c) and were associated with the AO and Pacific–North American (PNA) indices, respectively. A strong AO climate pattern characterized the late 1980s and early 1990s (Fig. 5.1), with associated temperature anomaly maxima in northern Europe and north-central Asia in winter (Fig. 5.3b), which expanded to northern Alaska in spring. As part of the positive AO pattern, west Greenland was anomalously cold. A positive PNA pattern was dominant from 1977 to 1988, with warm temperature anomalies over northern North America (Fig. 5.3c). The contrast of recent near-surface temperature anomalies, with maxima in west Greenland and northeast Siberia, to the temperature patterns associated with the AO and PNA suggest that the current atmospheric circulation pattern is also different from the main patterns of the second half of the twentieth century (Overland and Wang 2005).

ii) Arctic Ocean

(i) Surface circulation regime

The circulation of the sea ice cover and ocean surface layer are closely coupled and are primarily wind driven. Data from satellites and drifting buoys indicate that the entire period of 2000–05 has been characterized by an anticyclonic circulation regime due to a higher sea level atmospheric pressure over the Beaufort Gyre, relative to the 1948–2005 mean. The dominance of the anticyclonic regime is consistent with the AO index, which has exhibited relatively low and fluctuating values since 1996 (Fig. 5.1).

(ii) Heat and freshwater content

In recent years the heat and freshwater content of the Arctic Ocean have changed dramatically relative

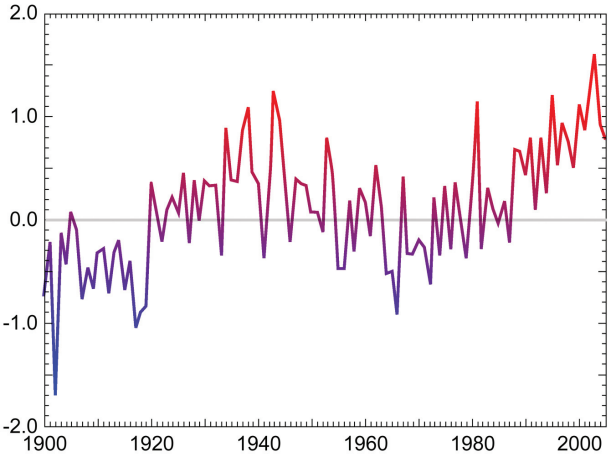

Fig. 5.2. Arctic-wide (60°N–90°) annual average surface air temperature anomalies (°C) over land for the twentieth century based on the Climate Research Unit (CRU) TEM2V monthly dataset.

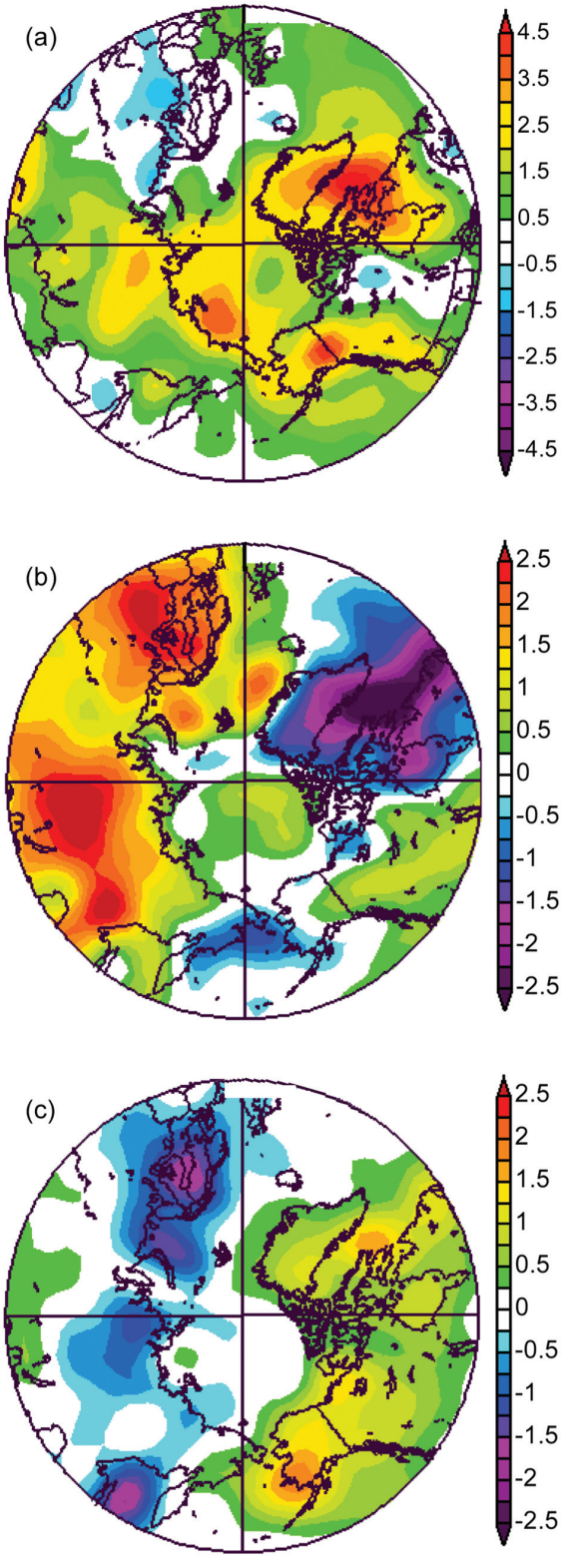

Fig. 5.3. 1000-hPa temperature anomalies (°C) for (a) March–June 2005 (relative to the 1968–98 mean), (b) December–March 1989–95, when the positive AO was strong, and (c) December–March 1977–88, when the positive PNA was strong. [Source: NCEP/NCAR reanalysis; online at www.ncdc.noaa.gov]

to averages established by the Arctic Ocean Atlas of the Arctic Climatology Project (1997), where water temperature and salinity from observations were averaged and gridded for the decades of the 1950s, 1960s, 1970s, and 1980s (Fig. 5.4). From 2000 to 2005, the western Arctic has been the focus of intensive investigation. This region includes the Beaufort Gyre, which is the major reservoir of freshwater in the Arctic Ocean. Although the total freshwater content in the Beaufort Gyre has not changed dramatically, there is a significant change in its distribution (Figs. 5.4c,d). The center of the freshwater maximum has shifted toward Canada and intensified relative to the average. Significant increases were also observed in the heat content of the Beaufort Gyre (Figs. 5.4a,b), primarily because of an approximately twofold increase of the Atlantic layer water temperature (Shimada et al. 2004).

The heat and freshwater content of the Arctic Ocean depends on inputs along open boundaries. The most important are fluxes in the Fram and Bering Straits. An increase of the Atlantic water temperature in the Fram Strait was observed in 2004 (Polyakov et al. 2005). In the Bering Strait region, preliminary observations from a mooring site, established and maintained since 1990, suggest that the annual mean water temperatures have been about a degree warmer since 2002, compared to 1990–2001. Since 2001, there has also been an increase in the annual mean transport. Combined, these changes have resulted in an increased northward heat flux through the Bering Strait in recent years (R. Woodgate, K. Aagaard, and T. Weingartner 2005, personal communication).

(iii)Sea level

There is a positive sea level trend along Arctic coastlines (Fig. 5.5). For 1954–89 the rate of sea level rise was estimated as +0.185 cm yr^{-1} (Proshutinsky et al. 2004). The addition of 1990–2004 data increases the estimated rate to 0.191 cm yr^{-1}. Arctic sea level also correlates relatively well with the AO index ($r = 0.83$). Consistent with the influences of AO-driven processes, Arctic sea level dropped significantly after 1990 and increased after the change from cyclonic to anticyclonic circulation in 1997. In contrast, from 2000 to 2004 the rate of sea level rise has increased in spite of a steady decrease in the AO index. At this point, because of substantial interannual variability, it is difficult to evaluate the significance of this change.

III) Sea ice cover

(i) Extent and thickness

During 2005, every month except May showed a record minimum sea ice extent in the NH relative

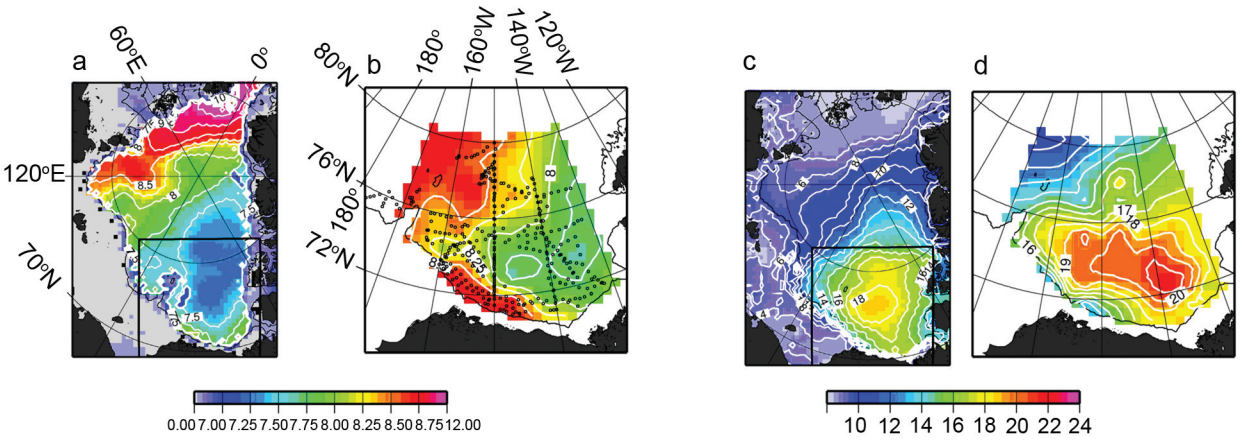

FIG. 5.4. Summer (a), (b) heat (x 10^{10} J m^{-2}) and (c), (d) freshwater (m) content. (a), (c) Heat and freshwater content in the Arctic Ocean based on 1980s averages (Arctic Climatology Project 1997). (b), (d) Heat and freshwater content in the Beaufort Gyre [outlined in black in (a) and (c)] in 2000–05 based on hydrographic surveys (black dots depict locations of hydrographic stations). Heat content is calculated relative to the freezing point in the upper-1000-m ocean layer. Freshwater content is calculated relative to reference salinity of 34.8 psu.

to the period 1979–2005 (J. Stroeve 2006, personal communication). This time period is defined by the availability of passive microwave images of sea ice extent in the NH. The extent of the sea ice cover is at or near its maximum in March and its minimum in September (Fig. 5.6). Ice extent in March 2005 was 14.8 million km^2, decreasing to 5.6 million km^2 in September 2005, compared to the mean (1979–2005) ice extent for March and September of 15.7 million km^2 and 6.9 million km^2, respectively. It is notable that in March 2005, ice extent fell within the mean contour at almost every location. In September 2005, the retreat of the ice cover was particularly pronounced along the Eurasian and North American coastlines.

To put the 2005 minimum and maximum ice extent into context, the variability of ice extent in March and September for the period of 1979–2005 is presented in Fig. 5.7. In both cases, a negative trend is apparent, with a rate of 2% $decade^{-1}$ for March and 7% $decade^{-1}$ for September. Furthermore, the summers of 2002–05 have experienced an unprecedented series of extreme ice extent minima (Stroeve et al. 2005).

Ice thickness is intrinsically more difficult to monitor. With satellite-based techniques only recently introduced, observations have been spatially and temporally limited (Laxon et al. 2003; Kwok et al. 2004). Data from submarine-based observations indicate that at the end of the melt season the permanent ice cover thinned by an average of 1.3 m between the period 1956–78 and the 1990s, from 3.1 to 1.8 m (Rothrock et al. 1999). On the other hand, measurements of the seasonal ice cover do not indicate any statistically significant change in thickness in recent decades (Melling et al. 2005; Haas 2004; Polyakov et al. 2003).

Trends in the extent and thickness of ice cover are consistent with observations of a significant loss of older, thicker ice out of the Arctic via the Fram Strait (e.g., Rigor and Wallace 2004; Pfirman et al. 2004; Yu et al. 2004) in the late 1980s and early 1990s. This event coincides with the strong, positive AO period from 1989 to 1995 (Fig. 5.1). When the AO is positive, atmospheric and oceanic conditions favor a thinner ice cover. A relatively younger, thinner ice cover, like the one left behind from this event, is intrinsically more susceptible to atmospheric or oceanic warming.

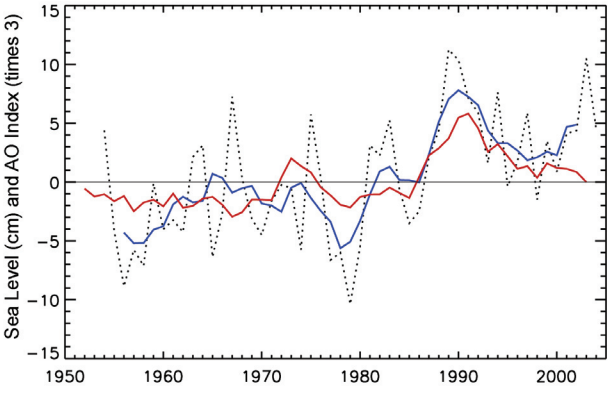

FIG. 5.5. Annual mean relative sea level (cm) from nine coastal tide gauge stations in the Siberian Seas (dotted line). The blue line is the 5-yr running mean sea level. The red line is the 5-yr running mean AO index (multiplied by 3 for comparison).

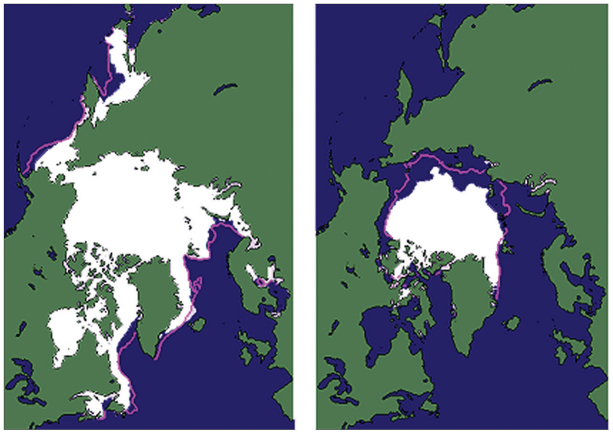

Fig. 5.6. Sea ice extent in (left) March and (right) September 2005, when the ice cover was at or near its maximum and minimum extent, respectively. The magenta line indicates the median maximum and minimum extent of the ice cover, for the period 1979–2000. [Source: NOAA/National Snow and Ice Data Center (NSIDC)]

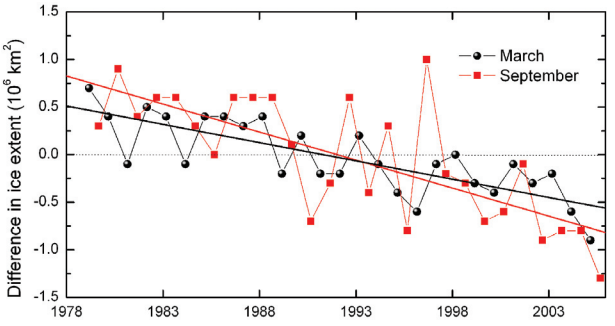

Fig. 5.7. Time series of the variability of ice extent in March (maximum) and September (minimum) for the period 1979–2005, normalized by the respective monthly mean ice extent for the period 1979–2005. Based on a least-squares linear regression, the rate of decrease in March and September was 2% decade^{-1} and 7% decade^{-1}, respectively.

(ii) Sea ice surface conditions

Data from 1982 to 2004, derived from AVHRR Polar Pathfinder extended (APP-x) products (updated from Wang and Key 2005a,b), indicate an overall negative trend for boreal summer (June–August) mean albedo of –0.4% yr^{-1} (Fig. 5.8a). The trend increases slightly to –0.5% yr^{-1} for the period from April through September (Fig. 5.8b), suggesting a possible increase in the duration of the melt season. In both cases, the surface albedo is relatively low from 2001 to 2004 and is consistent with observations of an earlier, more spatially extensive onset of melt and decrease in ice concentration (Belchansky et al. 2004, Stroeve et al. 2005).

The time series of APP-x annual mean skin temperatures (Fig. 5.8c) over the same period shows less consistent change over time, with a general increase in annual mean temperatures through the early 1990s and a decrease from 1995 onward. When the time series is limited to boreal spring (March–May) temperatures, the 23-yr linear trend is positive (0.14°C yr^{-1}), with greater interannual variability (Fig. 5.8d), indicative of the seasonal dependence of warming trends.

Large regional variability, typical of Arctic conditions, is observed in albedo, skin temperature, and ice concentration (Cavalieri et al. 1996). From 1996 to 2004, the largest decreases in surface albedo correspond to a reduction in ice extent in the Beaufort and Chukchi Seas. Lower albedos over the central ice pack appear consistent with the lower total ice concentrations over this same period.

IV) LAND

(i) Vegetation

The most convincing evidence of widespread change in Arctic vegetation comes from the historic

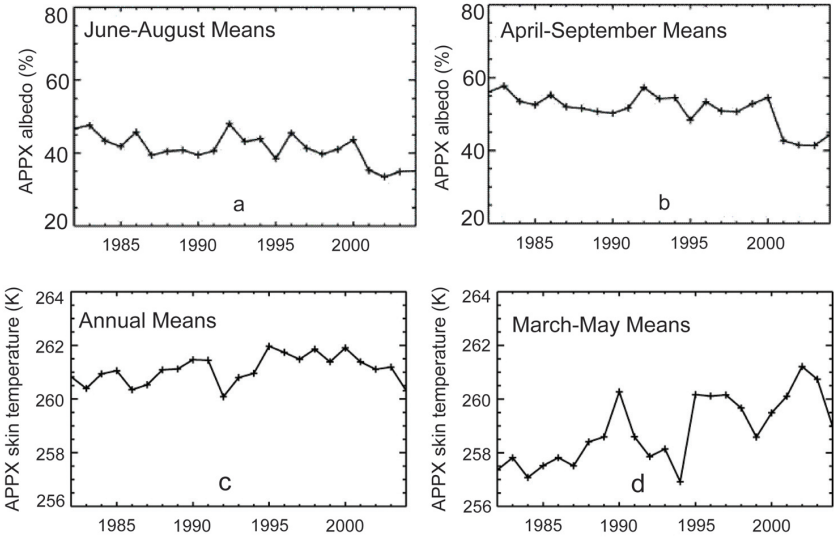

Fig. 5.8. APP-x (a), (b) surface albedo and (c), (d) skin temperature for areas between 60°N and 90° and ice concentrations of 15%–100% averaged over (a) June–August, (b) April–September, (c) January–December, and (d) March–May through 2004.

trends of tundra greenness as detected from satellites. The NDVI is a measure of vegetation greenness derived from surface reflectance in the red and near-infrared wavelengths. Higher-latitude NDVI values might be expected to increase under a warmed climate. Earlier global studies of NDVI changes indicated a general pattern of increased NDVI in the region between 40° and 70°N during the period of 1981–99 (Myneni et al. 1997, 1998; Zhou et al. 2001; Lucht et al. 2002). Studies of the NDVI indicate an increase of 17% in NDVI values in the tundra area of northern Alaska where the summer warmth index (SWI) values at meteorological stations have been increasing by 0.16° to 0.34°C yr^{-1} (Fig. 5.9) during the same period (Jia et al. 2003).

A more recent analysis covering the boreal forest and tundra region of North America indicates that different patterns of greening have occurred in the boreal forest and tundra areas (Goetz et al. 2005). The NDVI has increased in tundra regions by an average of about 10% for all of North America, whereas the NDVI has declined in the boreal forest regions particularly during the past 10 years.

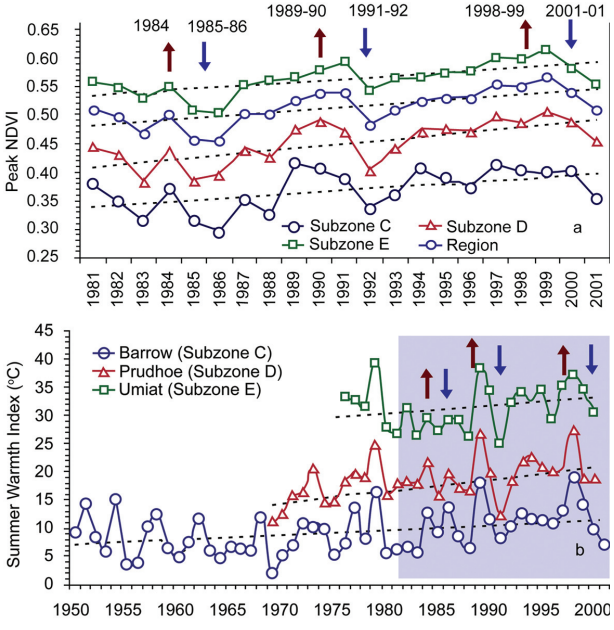

Fig. 5.9. (a) Peak NDVI derived from 8-km-resolution AVHRR data from 1981 to 2001 among the bioclimate subzones and for the whole Arctic slope. (b) Summer warmth index (SWI; °C) over the past 22–50 years at meteorological stations in each bioclimate subzone. Dashed lines are linear regressions. The shaded area in (b) highlights the period of SWI covered by the NDVI data in (a). The arrows show years of corresponding increases (red) and decreases (blue) in NDVI and SWI (from Jia et al. 2003).

(ii) Water

The R-ArticNet river discharge database (available online at www.R-Arcticnet.sr.unh.edu) was extended up to 2004 for 48 downstream river gauges. The last 5 years were characterized by an increase of total discharge to the Arctic Ocean mainly due to a contribution from Asian rivers. Mean 2000–04 discharge from Asia was 110 km^3 (5%) higher than over the previous 20 years. The mean discharge to the ocean from North America and Europe for 2000–04 was practically unchanged relative to 1980–99. A consistent increase in river discharge is observed from Eurasia for a longer time interval as well. The maximum total discharge of the six largest Eurasian rivers over 1936–2004 was observed in 2002, at 2080 km^3 yr^{-1} (Fig. 5.10). Mean discharge over 2000–04 for the large Eurasian rivers was 3%–9% higher than the discharge over 1936–2004. Thus, the contemporary data further confirm the presence of a significant increasing trend in the freshwater discharge to the Arctic Ocean from Eurasia documented earlier by Peterson et al. 2002 (Fig. 5.10).

(iii)Permafrost

Observations show a general increase in permafrost temperatures during the last several decades in Alaska (Osterkamp and Romanovsky 1999; Romanovsky et al. 2002; Osterkamp 2003), northwest Canada (Couture et al. 2003; Smith et al. 2003), Siberia (Pavlov 1994; Oberman and Mazhitova 2001; Romanovsky et al. 2002; Pavlov and Moskalenko 2002), and Northern Europe (Isaksen et al. 2000; Harris and Haeberli 2003). Uninterrupted permafrost temperature records over more than 20 years have been obtained by the University of Alaska–Fairbanks along the International Geosphere–Biosphere Pro-

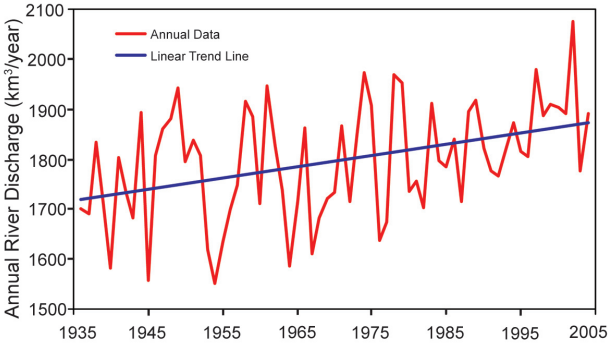

Fig. 5.10. Total annual discharge (km^3 yr^{-1}; red) to the Arctic Ocean from the six largest rivers in the Eurasian pan-Arctic for the observational period 1936–2004 (updated from Peterson et al. 2002). The least squares linear increase (blue) was 2.3 (km^3 yr^{-1}) yr^{-1}.

gramme (IGBP) Alaskan transect, which spans the entire continuous permafrost zone in the Alaskan Arctic. All observatories show a substantial warming during the last 20 years. This warming varied by location, but ranged typically from 0.5° to 2°C at the depth of zero seasonal permafrost temperature variations (Fig. 5.11).

These data also indicate that the increase in permafrost temperatures is not monotonic. During the observational period, relative cooling has occurred in the mid-1980s, in the early 1990s, and then again in the early 2000s. As a result, permafrost temperatures at 20-m depth experienced stabilization and even a slight cooling during these periods. An even more significant cooling of permafrost was observed during the very late 1990s and the early 2000s in interior Alaska. A significant portion of this cooling is related to a shallower-than-normal winter snow cover during this period. During the last three years, there was a sign of recovery in mean annual temperatures at shallow depths. Soil temperatures in interior Alaska during 2005 reached the temperatures of the early to mid-1990s, which were the warmest from during the last 70 years.

Data on changes in active layer thickness (ALT) in the Arctic lowlands are less conclusive. In the North American Arctic, ALT experiences substantial interannual variability, with no discernible trends; this is likely due to the short length of historical data records (Brown et al. 2000). A noticeable increase in the active layer thickness was reported for the Mackenzie Valley (Nixon et al. 2003). However, this positive trend became negative at most of these sites after 1998 (Tarnocai et al. 2004). An increase of more than 20 cm in thickness between the mid-1950s and 1990, derived from the historical data collected at Russian meteorological stations, was reported for the continuous permafrost regions of the Russian Arctic (Frauenfeld et al. 2004; Zhang et al. 2005). At the same time, reports from several specialized permafrost research sites in central Yakutia show no significant changes in the ALT (Varlamov et al. 2001; Varlamov 2003). The active layer was especially deep in 2005 in interior Alaska. Around Fairbanks, the 2005 active layer depth was the deepest observed in the past 10 years. Data from many of these sites show that the active layer that developed during the summer of 2004 (one of the warmest summers in Fairbanks on record) did not completely freeze during the 2004/05 winter. A thin layer just above the permafrost table remained unfrozen during the entire winter.

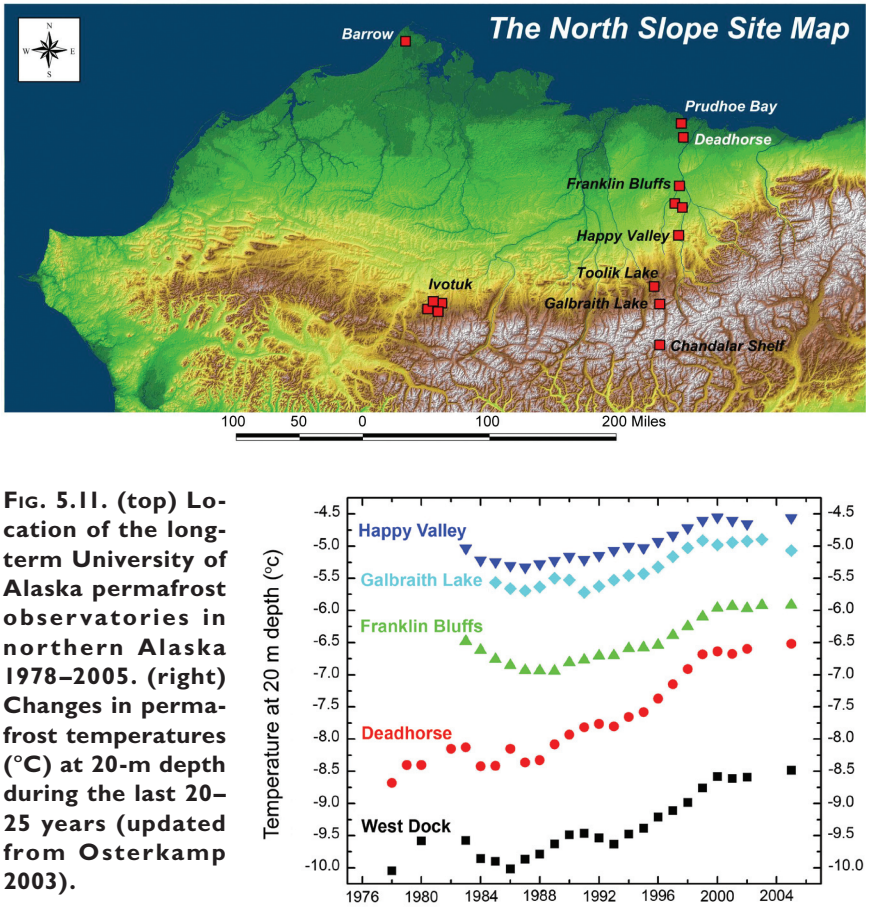

Fig. 5.11. (top) Location of the long-term University of Alaska permafrost observatories in northern Alaska 1978–2005. (right) Changes in permafrost temperatures (°C) at 20-m depth during the last 20–25 years (updated from Osterkamp 2003).

v) Greenland—J. E. Box[10]

(i) Overview

Temperatures in 2005 around Greenland were anomalously warm, particularly in boreal spring. In the period of record that includes three stations that began observations in the late 1800s, mean 2005 temperatures are rivaled only by recent years (e.g., 2003) and by warm conditions during the 1930s/40s. Unprecedented spring coastal fog caused flight delays along western Greenland that made European headlines. Widespread positive sea surface temperature anomalies surrounded Greenland for all seasons of 2005, according to the NOAA

SST OI version 2 (OIV2) dataset (1982–2005; available online at www.cdc.noaa.gov/cdc/data.noaa.oisst.v2.html). Upper-air temperature soundings available from the NCDC Integrated Global Radiosonde Archive (IGRA; Durre et al. 2006) indicate a pattern of tropospheric warm and stratospheric cool anomalies over Greenland, particularly in boreal winter.

(ii) Coastal temperature records

Although the coastal location of most meteorological stations makes it difficult to construct a representative climatology of temperature for Greenland, the existing 55-yr (1951–2005) record allows the annual mean temperatures of 2005 to be placed into historical context being as among the warmest, if not the warmest, on record (Table 5.1; see also Fig. 6.30). In northeast Greenland (Danmarkshavn) winter temperatures were among the warmest on record (99th percentile). Boreal spring was also unusually warm. Annual mean temperatures at all stations fell within the warmest decile (10%) of a normal distribution.

(iii)Greenland Ice Cap

Due to the paucity of regular observations of the Greenland Ice Cap, analysis of its behavior must necessarily be estimated by numerical modeling. Polar fifth-generation Pennsylvania State University (PSU)–National Center for Atmospheric Research (NCAR) Mesoscale Model (MM5) calculations (Box et al. 2006) indicate that increases in ice sheet melting exceeded increased snow accumulation in 2005, yielding a large (76%) negative surface mass balance anomaly (Table 5.2). In addition to precipitation increases, more of the precipitation was solid, despite a 1°C overall warm anomaly, suggesting that the upper elevations of the ice sheet received more snowfall than usual. Evaporation rates were 30% greater than normal, driven by warmer-than-normal average air temperatures. Blowing snow sublimation was slightly below normal due to decreased snow entrainment by the wind as a result of increasing melt duration (i.e., 10 days on average for the area below equilibrium line altitude). Meltwater production was 40% above normal owing to elevated summer temperatures and low-albedo positive feedback, which was particularly strong in August. Runoff rates were 45% above normal. Because of an apparent expansion of the ablation zone in this simulation, the accumulation area ratio was 7% below that of the most recent 17 years.

Previous observations have demonstrated accelerated ice sheet dynamic flow during surface melt water production (Zwally et al. 2002). Remote sensing measurements indicated widespread increases in glacier velocity south of 70°N (Rignot and Kanagaratnam 2006), confirming that flow rates did in fact increase in 2005. This suggests a Greenland Ice Sheet contribution to sea level that explains at least one-third of the observed recent accelerating global sea level rise (Leuliette et al. 2004).

c. Antarctic

1) ATMOSPHERIC CIRCULATION—A. Arguez[3]

The Southern Hemisphere annular mode (SAM; also known as the Antarctic Oscillation) is the Arc-

TABLE 5.1. Greenland station temperature statistics: 2005 versus 1951–2005.

Station Region	Location	Statistic	Winter	Spring	Summer	Autumn	Annual
Egedesminde	68.7 N	Rank	13	1	2	13	3
Central-west	52.8 W	*Z* score	–1.5	2.2	0.8	–0.1	1.9
Nuuk	64.2 N	Rank	N/A	1	10	19	N/A
Southwest	51.8 W	*Z* score	N/A	2.3	–1.4	0	N/A
Prins Christian Sund	60.0 N	Rank	7	1	1	17	1
South	43.2 W	*Z* score	–0.7	3.3	2.6	–0.3	2.4
Tasiilaq	65.6 N	Rank	7	2	2	34	3
Southeast	37.6 W	*Z* score	0.6	2.1	0.9	–1.1	3.2
Danmarkshavn	76.8 N	Rank	1	4	6	26	1
Northeast	18.7 W	*Z* score	2.8	–0.1	–0.8	0	2.6

Table 5.2. Greenland ice sheet surface mass balance parameters: 2005 departures from 1988 through 2004 average.

	% of 1988–2004 average	2005 minus 1988–2004 average [$km^3\ y^{-1}$]*
Total precipitation	110%	73
Liquid precipitation	107%	2
Evaporation	130%	21
Blowing snow sublimation	98%	–1
Snow accumulation	108%	52
Meltwater production	140%	238
Meltwater runoff	145%	206
Surface mass balance	24%	–153
Mean temperature	—	1.0°C
Accumulation area ratio	93%	–0.06

* Unless otherwise indicated.

tic Oscillation's (or Northern Hemisphere annular mode's) counterpart in the Southern Hemisphere. It is defined as the leading mode of 700-hPa height anomalies south of 20°S. Since early 2003, SAM positive and negative phase events have been uncharacteristically weak and ephemeral. During 2005, SAM values were fairly small except for a value of +1.2 in February and a considerably negative reading (–2.0) in December. However, weak values prevailed during the austral winter (Fig. 5.12).

ii) Temperature—A. M. Waple[89]

Surface air temperatures across the majority of stations on the Antarctic continent were near to above average in 2005, with the largest warming trends over the last several decades measured along the Antarctic Peninsula, for example, at the Rothera meteorological station (Fig. 5.13). Observed trends across the rest of the continent have been mixed, with interior stations such as Amundsen–Scott South Pole Station and Vostok showing small, significant trends in surface temperature. Not surprisingly, many stations in Antarctica are located near the more accessible coast and, therefore, deriving a representative continental temperature is virtually impossible. From the available temperature data, it is, perhaps, Antarctica's apparent continentwide temperature stability that is remarkable in the context of global warming. Only the Antarctic Peninsula (4% of the continental area)

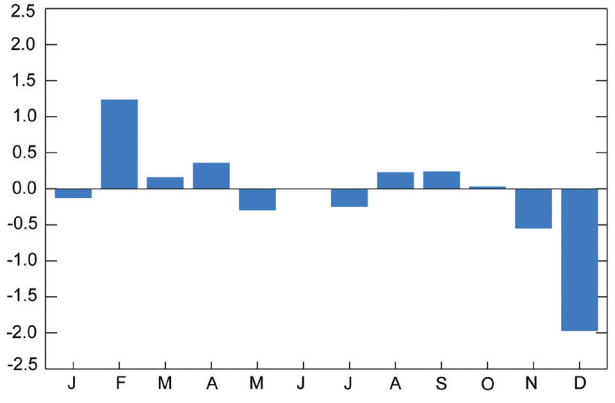

Fig. 5.12. Monthly values of the Southern Hemisphere annual mode index for 2005 (June value is missing).

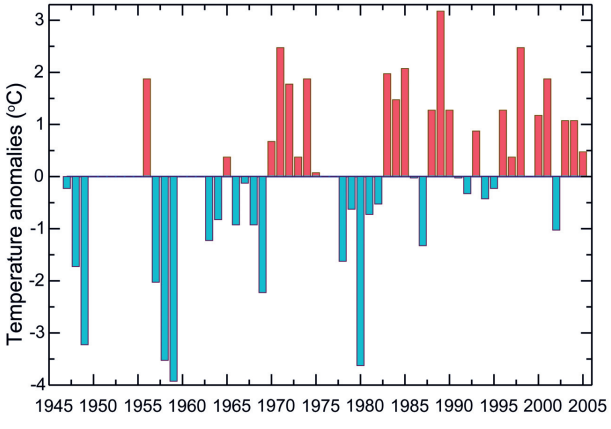

Fig. 5.13. Annual temperature anomalies from Rothera Meteorological Station on the Antarctic Peninsula. Base period is 1947–2005 and years without bars indicate unavailable data.

shows a significant warming trend. The peninsula is also the warmest area of the continent on average, rising above freezing for 2 months a year on its warmest coast (see information online at www.antarctica.ac.uk/About_Antarctica/Above_Antarctica/Weather/Temperature/index.php). Due to the paucity of stations on Antarctica, the lack of long-term records, and the high interannual temperature variability, it is impossible to state with certainty whether the Antarctic continent is warming or cooling overall. However, despite the lack of any clear warming signal in most coastal stations, there are indications that ice sheet thinning is occurring in west Antarctica and is considered a likely result of reduced buttressing by coastal ice shelves, which are melting or disintegrating, perhaps in response to coastal warming (e.g., Levinson 2005).

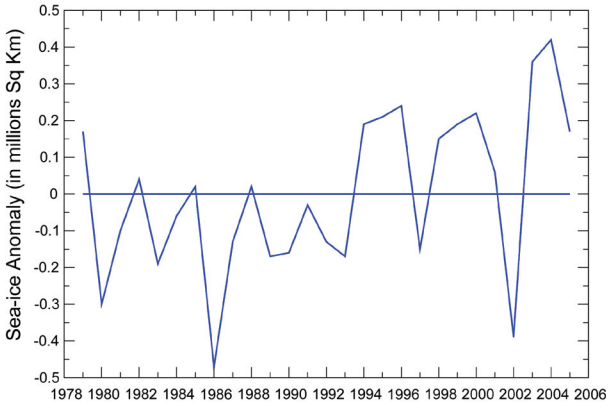

Fig. 5.14. Annual anomalies of Southern Hemisphere sea ice. Base period is 1979–2005. [Source: NOAA/NSIDC]

iii) Sea ice—A. M. Waple[89]

Southern Hemisphere sea ice extent has been increasing since the late 1970s (Fig. 5.14), with above-average extent in 2005. However, seasonal and spatial variability has been extreme in the Southern Hemisphere, with ice shelf and sea ice retreat occurring in those areas that have shown a warming trend over the last 50 years, such as the Antarctic Peninsula and Bellingshausen Sea (e.g., Vaughan and Doake 1996). The collapse of the Larsen A and Larsen B ice shelves in 1995 and 2002, respectively, indicate that pronounced regional warming can lead to ice shelf collapse and to glacial acceleration (Waple and Rignot 2005).

iv) Stratospheric Ozone—R. C. Schnell[81]

This year, 2005, was the 20th consecutive year of NOAA ozonesonde measurements at the Admunsen–Scott South Pole Station, and the NOAA/ESRL/Global Monitoring Division launched 68 balloon-borne ozonesondes in 2005. Figure 5.15a shows the total column ozone (blue line) in Dobson units and 20–24-km stratospheric temperature (red line), illustrating the development of the ozone hole over South Pole Station in 2005. The severity of ozone depletion depends on wintertime stratospheric temperatures, the stability of the polar vortex, and active chlorine levels. July and August profiles showed typical cold temperatures throughout the lower stratosphere, reaching a minimum of –92.3°C (180.9 K) on 10 July. The cold temperatures provided favorable conditions for the formation of polar stratospheric clouds that enable the transformation of Cl and Br compounds into species that destroy O_3 when sunlight returns to the Antarctic stratosphere. Total column O_3 remained stable until mid-August (Fig. 5.15b). Stratospheric O_3 declined to a minimum of 110 DU on 29 September, and was nearly completely destroyed in the 15–21-km layer (Fig. 5.15c). Compared to the years since 1986, 2005 was the 10th lowest for O_3 levels on record, with the record being 89 DU on 6 October 1993. Ozone abruptly increased to 333 DU on 13 November 2005 (Fig. 5.15d), due to midlatitude ozone-enriched air transported over the continent after the polar vortex began to break up.

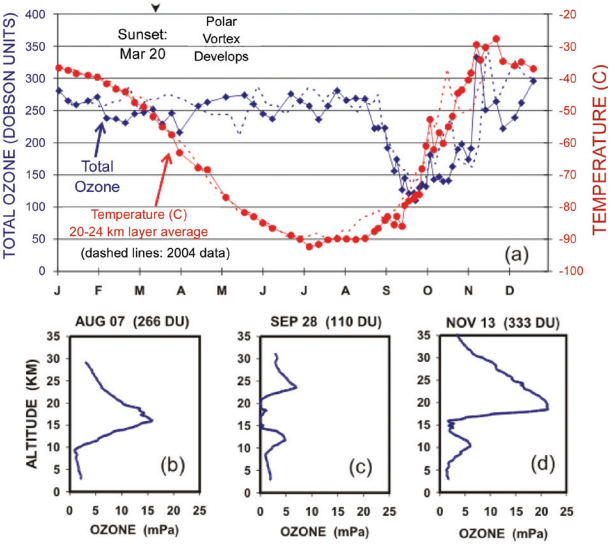

Fig. 5.15. (a) Summary of South Pole total ozone in Dobson units and stratospheric temperatures measured by ozonesondes during 2005. Three selected profiles of altitude vs ozone partial pressure (mPa) are shown (b) prior to the 2005 ozone hole, (c) at minimum total ozone, and (d) postozone hole. [Source: B. Johnson and S. Oltmans, NOAA/ESRL/GMD]